

Screening of Carbofuran-Degrading Bacteria *Chryseobacterium* sp. BSC2-3 and Unveiling the Change in Metabolome during Carbofuran Degradation

Haeseong Park ¹, Sun Il Seo ¹, Ji-Hwan Lim ¹, Jaekyeong Song ², Joo-Hyun Seo ^{3,*} and Pyoung Il Kim ^{1,*}

¹ Center for Industrialization of Agricultural and Livestock Microorganisms, 241 Cheomdangwahak-ro, Jeongseup-si, Jeollabuk-do 56212, Korea; haeseong@cials.or.kr (H.P.); siseo@cials.or.kr (S.I.S.); ljh0408@cials.or.kr (J.-H.L.)

² Division of Agricultural Microbiology, National Academy of Agricultural Science, Rural Development Administration, Jeonju 56050, Korea; mgjksong@korea.kr

³ Department of Bio and Fermentation Convergence Technology, Kookmin University, Seoul 02707, Korea

* Correspondence: joohyunseo@kookmin.ac.kr (J.-H.S.); pikim30@cials.or.kr (P.I.K.); Tel.: +82-63-536-6001 (P.I.K.)

Table S1. General features of the *Chryseobacterium* sp. BSC2-3 genome.

Characteristic	Genome	Characteristic	Genome
Genome size (bp)	4786171	Mean of CDS length (bp)	980.5
GC content (%)	36.8	Median of CDS length (bp)	804
Number of contigs	14	Mean length of intergenic region	135.2
Number of CDSs	4312	Number of rRNA genes	6
N50 (bp)	503816	Number of tRNA genes	80

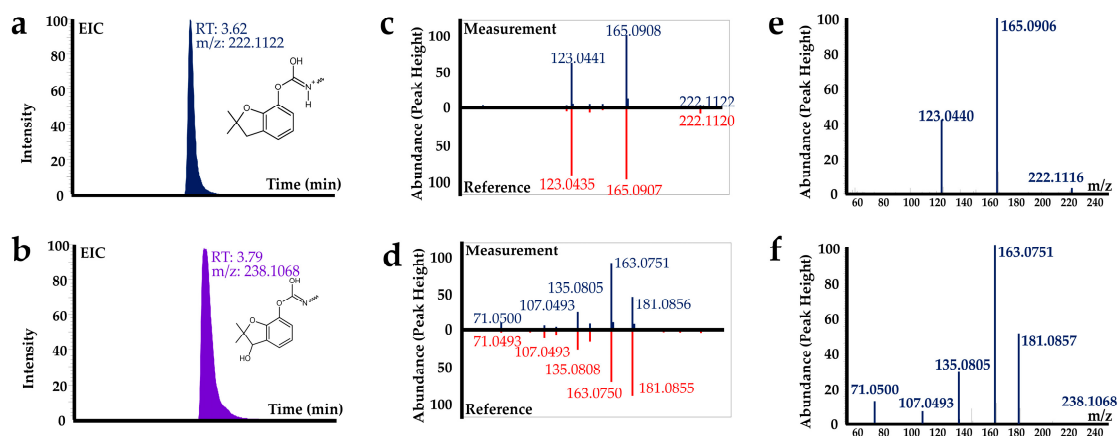


Figure S1. Extracted ion chromatograms (EICs) of the target compounds carbofuran (**a**) and 3-hydroxycarbofuran (**b**) in positive ionization mode. The mirror plot represents the concordance of MS/MS fragments of standard (up-blue) and library (down-red) in carbofuran (**c**) and 3-hydroxycarbofuran (**d**). Mass fragment spectral results of carbofuran (**e**) and 3-hydroxycarbofuran (**f**) in the real samples

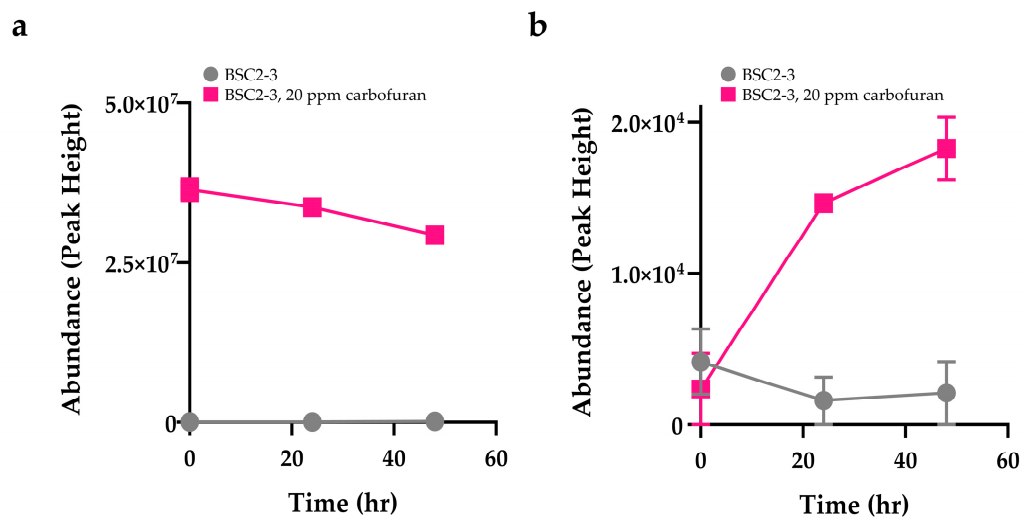


Figure S2. The graph shows the changes in the relative abundance of carbofuran (a) and 3-hydroxycarbofuran (b) in the supernatant in a time-dependent manner

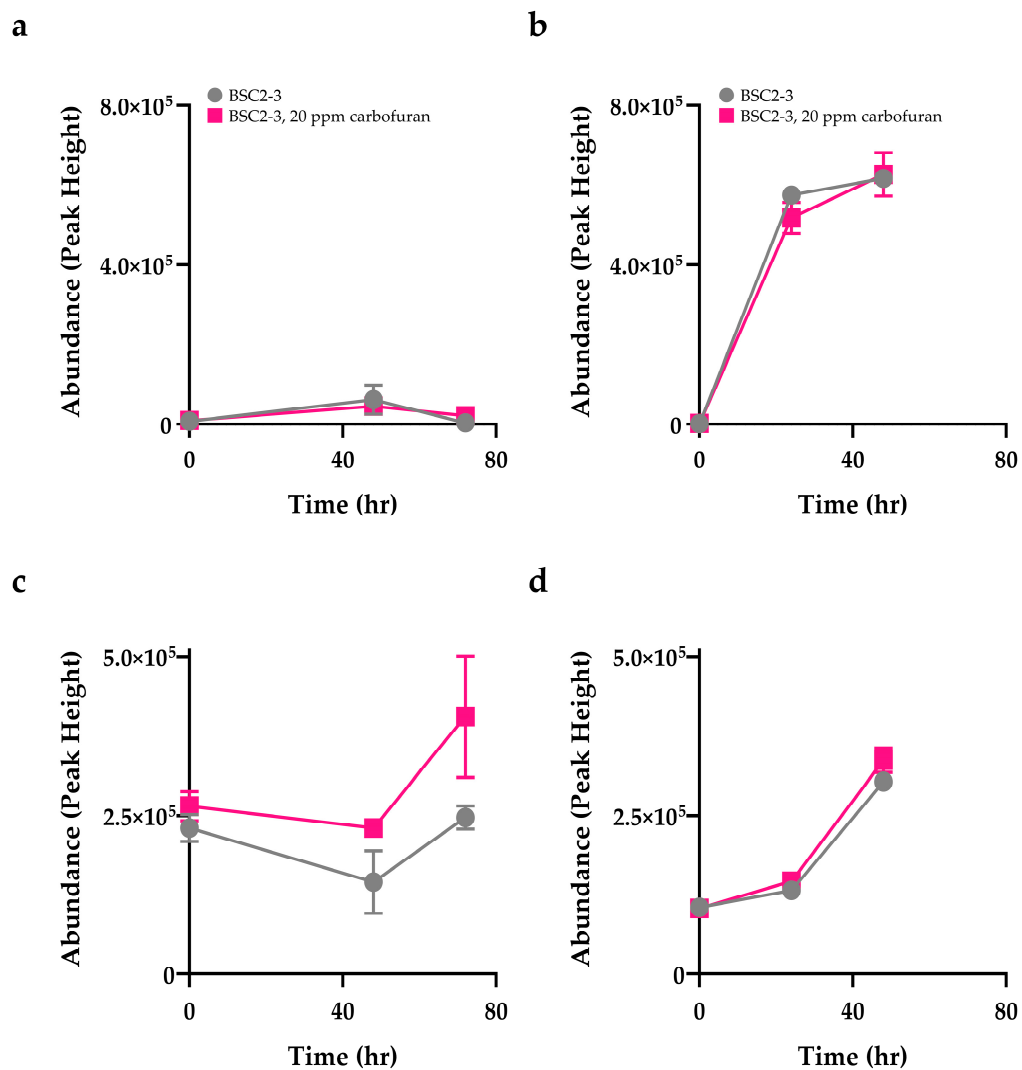


Figure S3. Alterations in the relative abundance of intracellular (a), (c) and extracellular (b), (d) riboflavin (a), (b) and lumichrome (c), (d) in a time-dependent manner

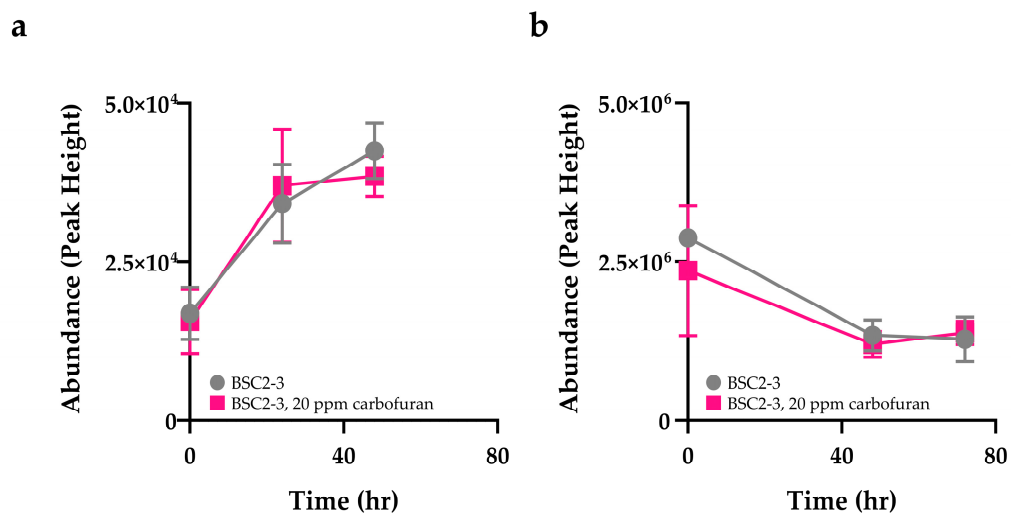


Figure S4. Time-course extracellular (a) and intracellular (b) changes in indole-3-acetic acid content